JOINT INSTITUTE FOR NUCLEAR RESEARCH
Veksler and Baldin laboratory of High Energy Physics

FINAL REPORT ON THE SUMMER STUDENT PROGRAM

Supervisor:
Elena Kokoulina

Student:
Fazilat Rasulova, Uzbekistan,
National Research Nuclear
University MEPhI

Participation period:
July 01 – August 17

Dubna, 2019

INTRODUCTION

Direct photons (DP) by definition are not products of decay of any known particles [1–3]. In accordance with quantum electrodynamics (QED) they may be emitted in the process of charged particle scattering, bremsstrahlung in a parton or hadron cascade. In particular, $q\bar{q} \to g\mathcal{g}$ and $gq \to \gamma q$ parton interactions lead to photon emission. The higher the density and the longer the system lifetime, the more DP should be emitted. The produced photons interact with the surrounding matter only electromagnetically, and therefore they keep information about the environment surrounding them during the whole history of evolution.

Special attention is devoted to low-energy DP, or soft photons (SP), whose experimental yield surpasses the theoretical predictions by 4–8 times [4–8]. This concerns K^+p and pp interactions at 70 GeV/c [4,5] as well as $\pi^{\pm}p$ and K^+p interactions at 250 and 280GeV/c [6–8]. The recent results on this subject by the DELPHI collaboration [9, 10] are devoted to studying SP inside hadronic jets originating in the process $Z^0 \to q\bar{q} \to$ jet + X. The authors claim that a clear excess of SP relative to a hadronic jet in comparison with the theoretical prediction gives a factor 3 when all particles in the jet are charged and a factor 17 when the jet includes only neutral particles.

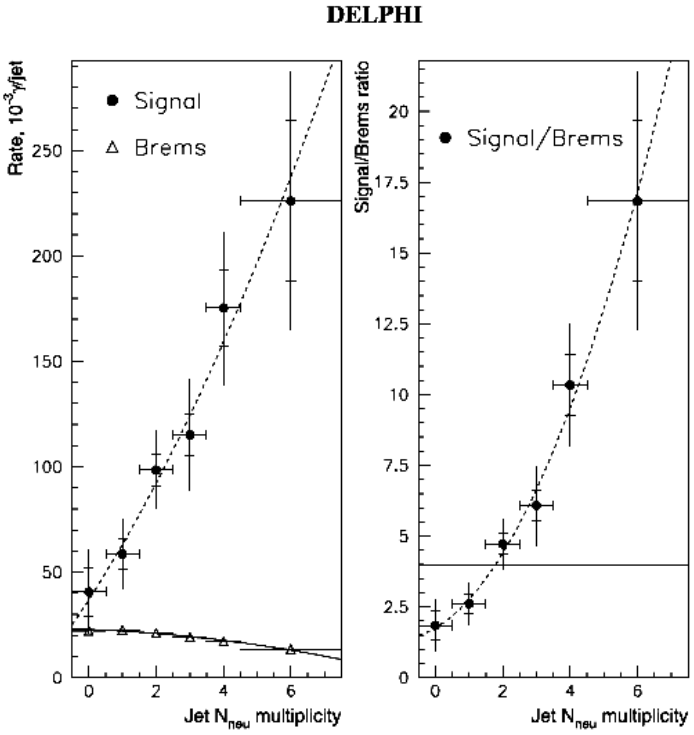

Figure.1. Dependence of the direct soft photon production on the jet neutral multiplicity. *Left panel:* signal and predicted inner bremsstrahlung rates as a function of the jet neutral multiplicity. *Right panel:* ratios of the signal rates to those of the inner bremsstrahlung

In fig. 1 the difference between the transverse momentum spectrum of SP and predictions of the Parton Shower Monte Carlo (MC) model are presented. Photons

emitted close by the jet axes are selected. The jet results from the decay $Z^0 \rightarrow$ jet + X. DELPHY data are used. Triangles show the bremsstrahlung spectrum calculated from QED [9, 10].

The SP surplus can be assigned to an unknown physical process. For qualitative explanation of this effect the assumption of the formation of a cold spot of quark-gluon plasma (QGP) or hadronic gas has been made in a number of theoretical models [11–14]. It is argued that a cold spot is relatively stable and radiates SP. These photons testify the existence of a new phenomenon connected with the collective behavior of particles, see for example [15].

In ref. [11] the formation of a cold zone of the QGP in a hadronic gas is assumed (model cQGP). The authors believe that cold partons don't have enough energy for hadronization. So they recombine in hadrons rather slowly. The cold QGP droplet has a big lifetime and it reveals itself as a source of low-energy DP. The idea of a cold spot of pion gas is considered in ref. [12]. Slow pions are repeatedly reflected from the border of hot and cold areas and have a large lifetime. Again at the cost of a long lifetime the cold spot radiates SP with low energy in the c.m.s.

A new interesting idea has been advanced in ref. [16] where the analogy between expanding hadronic fireball and expanding universe was supposed. In both cases the spectrum and intensity of emerging photons can be described by a black-body radiation formula. DP appears as an analogue of the cosmic microwave background radiation. A semi-qualitative description of the available experimental data has been achieved. In accordance with a gluon dominance model (GDM) [17–23] the energy of colliding hadrons is transformed to the energy of initial particles and a formed quark-gluon system. This model describes well the high multiplicity region [24]. Half of the active gluons (about 47%) produce hadron jets and the remaining gluons can be sources of SP.

The study of SP spectra seems especially interesting for the future accelerator complex NICA [25] as it aims to deal with a high-density system [26,27]. The goal of the SP study experiment is the investigation of collective behavior of particles in the process of multiple hadron production in pp, pA and AA interactions at the colliding beam energy $E \approx 5$ GeV per nucleon. The domain of high multiplicity (central collisions) will be interesting for SP study depending on the multiplicity of charged or neutral secondary particles. We hope studying the dependence of the SP yield of on the multiplicity of charged and neutral particles. Using electromagnetic calorimeters we can search for new states of neutral particles, study interference of SP and solve other tasks [28].

SP CALORIMETRY

Electromagnetic calorimeters (ECal) are detectors in which the impinging photons and electrons lose (ideally) all their energy, part of which is converted into some detectable signal. The energy loss mechanism is the production of secondary particles in an alternating sequence of pair creation ($\gamma \rightarrow e^+e^-$) and Bremsstrahlung ($e^{\pm} \rightarrow e^{\pm}\gamma$), until the energy of the secondary fall below the

critical energy [29]. The set of secondary is the (electromagnetic) shower, a statistical object. The average depth of the shower is proportional to ln(E), and is usually measured in units of radiation length X_0 (related to the mean free path of the shower particles in the material), while the transverse size is characterized by the Moliere-radius ρ_M (about 95% of the electromagnetic shower is contained laterally in a cylinder with radius $2\rho_M$ [29]). Part of the deposited energy is converted into some detectable signal, like Cerenkov or scintillation light, captured by some photo-sensitive device, or the number of electrons at various depths, typically measured by silicon detectors. The transverse size of the detector modules read out individually (granularity) is of the order of ρ_M , optimizing the contradictory requirements of energy and position resolution. To prevent shower leakage at the far end the depth of the modules should be at least $18\text{-}20X_0$.

Calorimeters can be homogeneous, like scintillating crystals or strong Cerenkov emitters; in these transparent detectors the entire volume is active, because light is produced everywhere and most of it can be collected and observed. In sampling calorimeters highly absorbing passive regions (usually high Z material) absorb most of the energy without producing detectable signals. These alternate with regions of active material, where the remaining energy of the shower produces observable light or charge ("visible energy"). The ratio of visible to total energy is called the sampling fraction. Due to the statistical nature of shower development the resolution of sampling calorimeters is inferior to homogenous ones, but they can be much more compact and cost-effective. For good calorimeters the resolution is dominated by the statistical term $\sigma_E/E \propto A/\sqrt{E(\text{GeV})}$, with A in the few percent range for homogenous and ≈ 8-15% for sampling calorimeters. Excellent reviews of calorimeter technologies, performance, applications (and pitfalls!) can be found in [29].

Photon reconstruction in ECal identifying showers (clusters in the raw data) that are likely coming from photons, rejecting hadrons, reconstructing the photon energy and its impact point on the calorimeter surface. An additional, extremely important step is at higher energies to determine whether a single, photon-like cluster comes indeed from a single photon, or two nearby photons, e.g. from a π^0 decay (merging). Hadron rejection is sometimes aided by a thin, charge-sensitive device in front of the calorimeter (charge veto), while the position measurement and the resolution of two nearby photons can be enhanced by a high granularity "pre-shower" detector. The principal tool for photon identification is the analysis of the shower shape (size, compactness, dispersion, ellipticity, in comparison to the predictions of a shower model etc.), where the different characteristics are often combined stochastically [29]. Another way to distinguish between single photons and merged decay photons of the same total energy is to use a longitudinally segmented calorimeter (see for instance the UA1 detector at CERN [88]): the penetration of the two smaller energy photons is shallower, so the ratio of energy deposit in the first and second segment discriminates between a single high energy

and two lower energy, but merged photons.

The direct photon signal has a large background from hadron decay photons. In a low multiplicity environment, like pp collisions, such decay photons can be tagged in each event with a reasonable efficiency by checking if it has an invariant mass $m_{\gamma\gamma}$ consistent with π^0 if combined with any other photon in the event. In high multiplicity events, for example in A+A interactions, such tagging isn't possible, because the combinatorial background is too large. In A+A the direct photon yield is usually obtained statistically, by subtracting the estimated decay photon yield from the observed inclusive yield. The decay kinematics is known, but it is hard to overemphasize how much in these type of measurements the accuracy of the final direct photon result depends on the knowledge of hadron yields, particularly those of π^0 and η. Ideally those are measured in the same experiment, with the same setup, to minimize systematic uncertainties from acceptance, absolute calibration, and so on. Note that the photon contribution from other meson decays is usually small compared to other uncertainties of the measurement.

Once the π^0 and η spectra are known, their decay photon contribution in the detector has to be simulated (including the acceptance and analysis cuts), then this simulated decay spectrum is subtracted from the inclusive photon spectrum. Finally, the difference (inclusive - decay), i.e. the direct photon spectrum has to be unfolded for detector resolution and other effects.

Interaction of particles with matter

When a particle reaches ECal, it interacts with the constituents of the matter, that is to say its atoms (electrons and nuclei). Depending on different factors (distance from the center, energy, charge, etc.), different interactions can occur. Generally, two main effects can happen: the particle can be absorbed or scattered. Both effects involve a loss of energy.

From a macroscopic point of view, the particle may be stopped (hence the stopping power of some materials), or slightly deflected (straggling) while pursuing its course, or even strongly deflected. Furthermore, the particle may not interact, interact once, or even interact more than once while passing through the matter.

However, as the exact position of the atoms in the material is not known, and the interactions described by quantum mechanics can only define probabilities of outcome, it is not possible to predict a priori what will happen for a given incoming particle impinging on the matter. The interaction of a particle with matter is then a highly statistical process. If this interaction is reproduced for a statistically significant number of incoming particles, the different global characteristics of the interaction can be observed.

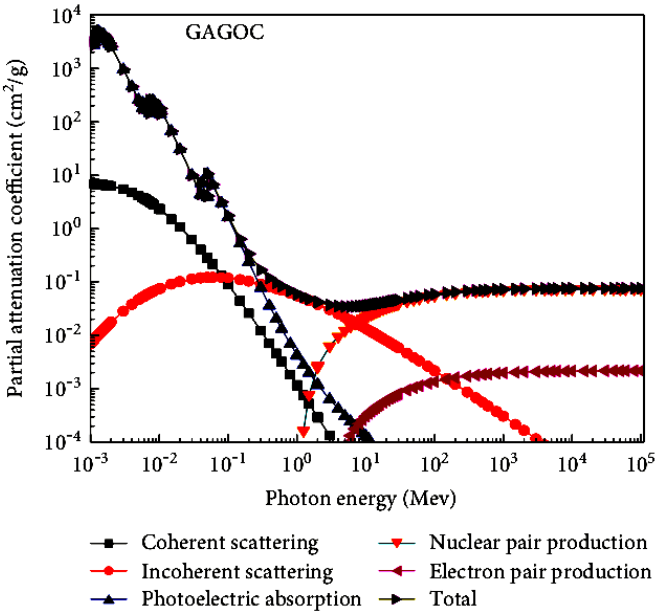

Figure 2: The photon absorption coefficient for a sample material (here: GAGOC) at different photon energies. Data Source: [30]

For photons, there are three main interaction processes with matter: the photoelectric effect, where a bound electron is excited to a state of higher energy, Compton scattering, in which a free (or weakly bound) electron collides with the photon and pair production, which means the photon produces an electron positron pair.

Each of these processes is strongly dependent on the specific material. Typically, the photoelectric effect is dominant at small energies in the keV range, Compton scattering dominates in the range from a few hundreds of keV to a few MeV, and governed by pair production above a few MeV.

Due to the high light yield, speedy decay time, high density, high Z_{eff}, and good energy resolution of GAGOC scintillator materials, it is a great nominee for many applications like gamma spectroscopy and position emission tomography (PET). Furthermore, GaGG:Ce does not have natural radioactivity.

When an incoming particle interacts with the scintillator, it can produce secondary particles, possibly forming a cascade of particles with successively less energy, which is called an electromagnetic shower. If the whole cascade is contained within the scintillator, all of the kinetic energy 5 of the incoming particle is be absorbed by the scintillator and the number of visible photons which will be emitted will be proportional to that energy.

The photons are then detected with a suitable detector, such as a photomultiplier tube or silicon PMT (SiPM) or – in the case of this experiment – an avalanche photodiode (APD). In a nutshell, the signal output from these devices serves as a measurement of the energy of the incoming particle. The APD current is proportional to the photon flux, and thus the integrated current – the charge – is proportional to the total number of photons emitted by the gadolinium-gallium-garnet (GaGG:Ce) – which in turn is proportional to the energy deposited in the crystal.

GEANT4 for SIMULATION

We use Geant4 for simulation and estimation of opportunity of sampling ECal for SP registration. Word Geant has the following abbreviation: GEometry ANd Tracking (version 4) [31]. It is a set of libraries providing tools to perform simulations. It is programmed in C++, and follows an Object-Oriented philosophy. The algorithms developed are based on the Monte-Carlo approach. The Monte-Carlo algorithm consists in repeating similar process but with randomized starting conditions or events. In our case, the emission directions of the photons (which we will provide to GEANT), as well as the different interactions that will take place (which GEANT will do for us) are obtained randomly. Geant has a rather long-standing history as the very first version of Geant was developed at CERN in 1974. In 1998, the fourth version of Geant was released in order to replace Geant3, which was programmed in FORTRAN (as part of CERNLIB). In 1999 it was adopted by the XMM collaboration in space physics, and then high-energy physics community adopted it too: Babar (2001), ATLAS, CMS or LHCb (2002). It is the de-facto standard for simulating particle-matter interactions in physics.

The structure of Geant4 operates around different components: material, geometry, physics lists, event generator, visualization and analysis. But before, the global organization of the code has to be presented.

1. Usercode

In order to simplify the programming part, a working simulation is provided as a starting point.

It is composed of the following parts:

- EmCal.cc: this is the main file of the program (which contains the main() function of the C++ code). It will be called when running the program, and is responsible for calling the other code.
- Makefile: this file is used for the compilation. In order to compile the program, one should simply type make in the directory.
- include: this directory contains the class/headers definitions. Header files give other parts of the code (such as EmCal.cc) information on how to interact with it. For example, EmCalDetectorConstruction.hh gives information on how to interface with the code written in the class EmCalDetectorConstruction.cc.
- src: this directory contains the sources definitions. Each class has a certain number of corresponding functions. For this lab course, only the files in this directory need to be modified.

The code organization is then summarized in Figure 3.

The simulation represents a certain geometry composed with specific material and following some physics rules. The simulation is a run on several events, each starting with the action of a given source, and following the different steps of interaction.

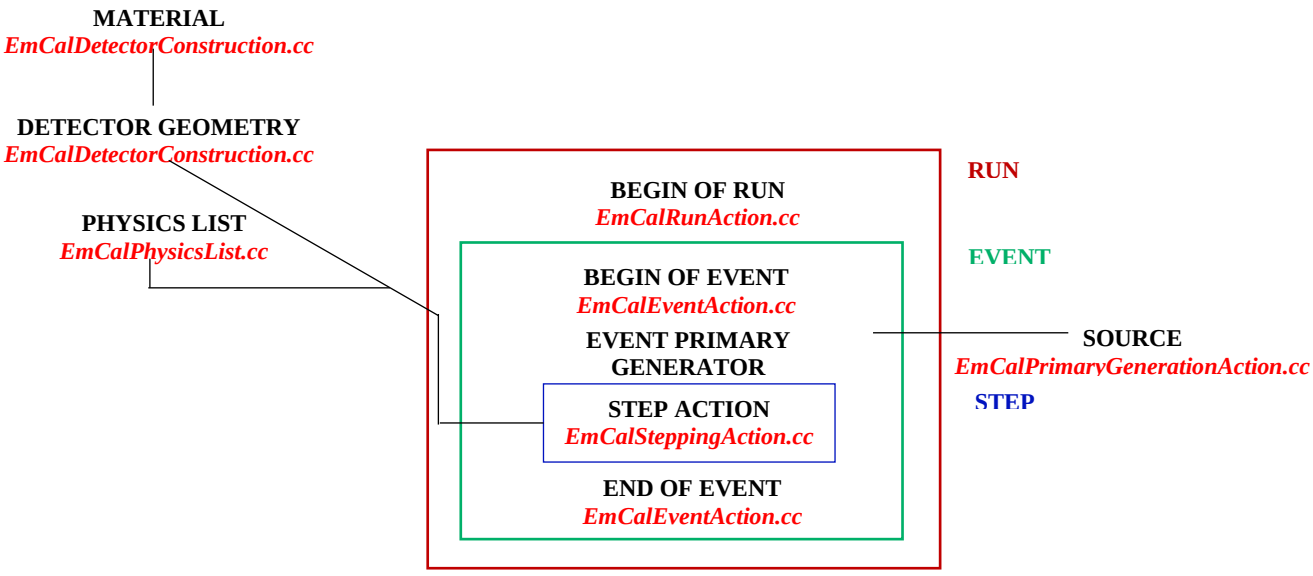

Figure 3: Summary of the different parts of the usercode program with details on the files used

2. Material

Geant4 allows for different definition of materials. The first and simplest way to define some material to be used in the simulation is by using the predefined library of Geant4 [32] as

```
G4Material* CsI = nist->FindOrBuildMaterial("G4_CESIUM_IODIDE");
```

One can also define some new element from the scratch as

```
G4Element* O = new G4Element(name="Oxygen" , symbol="O" , z= 8., a= 16.00*g/mole);
G4Element* Ga = new G4Element(name="Gallium" , symbol="Ga" , z= 31., a=
69.723*g/mole);
G4Element* Gd = new G4Element(name="Gadolinium" , symbol="Gd" , z= 64., a=
157.25*g/mole);
```

Also we can define more complex material using, $Gd_3Al_2Ga_3O_{12}$:Ce.
In the code on which you will be working, the material is defined in the file EmCalDetectorConstruction.cc.

3. Geometry

The building of the geometry is composed of different definitions: solids, logical volumes and physical volumes. On the top, there is a special volume, in which all the others are placed (experimental hall). As the material, the geometry is defined in EmCalDetectorConstruction.cc.

Figure 3 gives an overview of the different steps necessary to create an actual physical volume:

First, a solid has to be defined. This is just an abstract geometrical object. Then, a solid and a material are used to create a logical volume. A logical volume can be though of the idea of (for example), a 1 cm 3 CsI cube. Figure 3 gives an overview of the different steps necessary to create an actual physical volume:

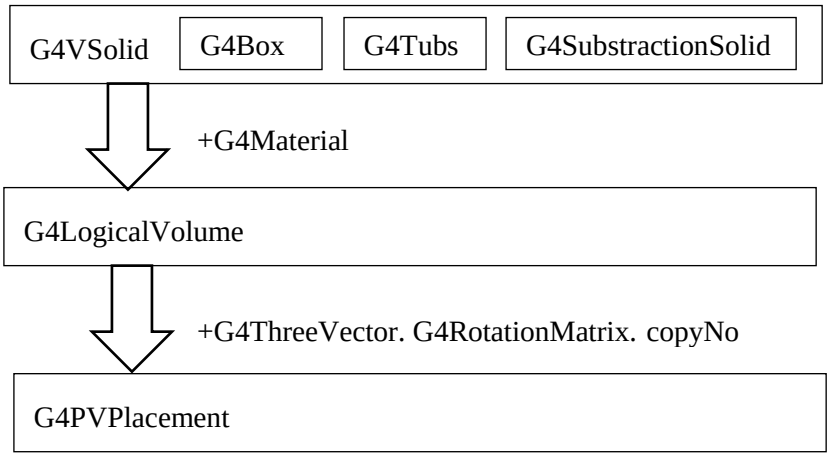

Figure 3. Steps to create a physical volume placement

First, a solid has to be defined. This is just an abstract geometrical object. Then, a solid and a material are used to create a logical volume. A logical volume can be though of the idea of (for example), a 1 cm 3 CsI cube.

Finally, to create an actual physical volume, one has to create a placement using the logical volume and a vector indicating the point in space where its center of mass should be. A logical volume can be placed multiple times, each time generating a different physical volume.

Solids

Geant4 offers the possibility to define different geometrical forms and methods to combine them in order to produce the solids that will be needed to build the detector.

A simple box can then be defined in the following:

```
G4double totSizeX  = 18.0*mm;
G4double totSizeY  = 18.0*mm;
auto calorimeterS = new G4Box("Calorimeter", totSizeX/2, totSizeY/2, calorThickness/2);

G4double fiberSizeX  = 1.0*mm;
G4double fiberSizeY  = 1.0*mm;
auto fiberS= new G4Box("fiber", fiberSizeX/2, fiberSizeY/2, calorThickness/2);
```

As you can see, for predefined Geant4 solids, the length are given relative to the center of mass. Similarly to the box, there are several others: G4Cons, G4Orb, G4Para, G4Sphere, G4Torus, G4Trap, G4Trd and G4Tubs. And those can be combined.

Logical volumes

From the solids defined, one can then define some logical volumes as

```
WorldLV = new G4LogicalVolume( worldS,          // its solid
                               defaultMaterial,  // its material
                               "World");         // its name
```

Essentially, it means to assign some material to one solid figure.

```
G4int nofParticles = 1;
fParticleGun = new G4ParticleGun(nofParticles)
auto particleDefinition = G4ParticleTable::GetParticleTable()->FindParticle("gamma");
fParticleGun->SetParticleDefinition(particleDefinition);
fParticleGun->SetParticleMomentumDirection(G4ThreeVector(0.,0.,1.));
fParticleGun->SetParticleEnergy(500.*MeV);
```

Physical volumes

Once the logical volumes have been defined, one can physically place them in the space using the function

```
fWorldPV= new G4PVPlacement( 0,               // no rotation
                             G4ThreeVector(),  // at (0,0,0)
                             worldLV,          // its logical volume
                             "World",          // its name
                              0,               // its mother  volume
                              false,           // no boolean operation
                              0,               // copy number
                              fCheckOverlaps);  // checking overlaps
```

Note that the position vector sets the position of the center of mass of the logical volume

4. Event generator

Now that the material, the geometry and the rules have been defined, the simulation can run.

Source

The first thing is to define the source of the event: what will happen which creates the event (incoming ion, etc.). This is made in EmCalPrimaryGeneratorAction.cc. And we use a simple photon generator as

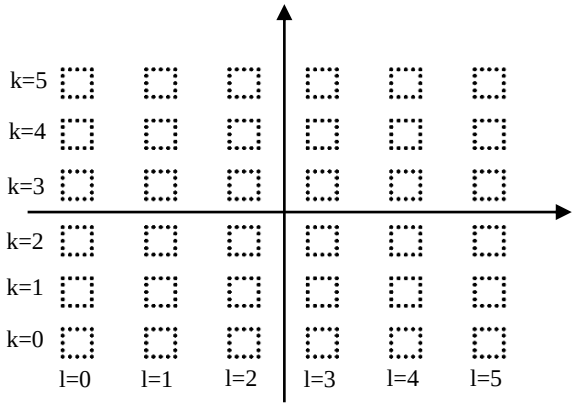

Figure 4. Cycle filling scheme

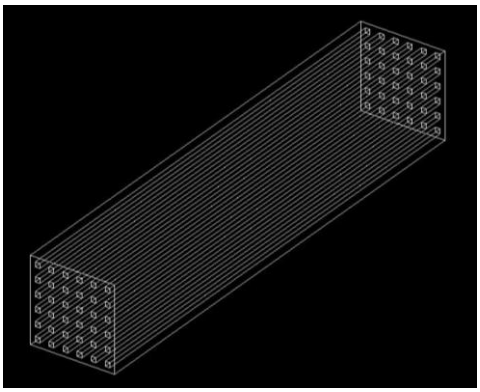

Figure 5. General view of calorimeter

Run

Afterwards the simulation can start. This is a run that is composed of several events. It is possible to have some actions at the beginning of the run as

```
void EmCalRunAction::BeginOfRunAction(const G4Run* /*run*/)

{
G4cout << "### Run " << aRun->GetRunID()<< " start." << G4endl;

fRootFout = new Tfile("test.root", "RECREATE", "My GEANT4 simulation");
fRootTree = new TTree ("tree","My GEANT4 simulation") ;
fRootTree->Branch("e",e,"e[100]/D") ;
}
```

defined in EmCalRunAction.cc. A new ROOT file is opened and a tree with 100 branches (maximal number of crystals) is created.

Event

Each event has four levels: beginning, event action generator, steps and end.

At the beginning of the event, one can initialize the variables that will be used, and at the end, the resolution of the detection can be applied, the energy of each detector stored in the ROOT tree. Both are defined in EmCalEventAction.cc. But the main part of the event is the event action generator. Using the source (and in EmCalPrimaryGeneratorAction.cc), the photon is emitted with an isotropic probability distribution.

Step

That photon, or more generally the particle(s) generated are sent through the experimental hall and until they interact with one of the constituents (matter). This is a step. Each step ends with either an interaction or when the particle leaves the experimental hall. Some action can be done at each step, in particular, collecting the energy deposit by the particle.

```
void EmCalSteppingAction::UserSteppingAction(const G4Step* step)
{
 auto edep = step→GetTotalEnergyDeposit();
 G4double stepLength = 0.;
 if ( step->GetTrack()->GetDefinition()->GetPDGCharge() != 0. ) {
 stepLength = step→GetStepLength();};
 fEventAction→AddTot(edep,stepLength);
}
```

The visualization working group develops and maintains the Geant4 systems for vizualizing geometries, trajectories and hits. These systems include the core visualization interfaces plus a large number of specific visualization drivers to provide a wide variety of graphics capabilities. The visualization working group advises users on how best to exploit the available tools and how to integrate Geant4 visualization into any pre-existing software framework.

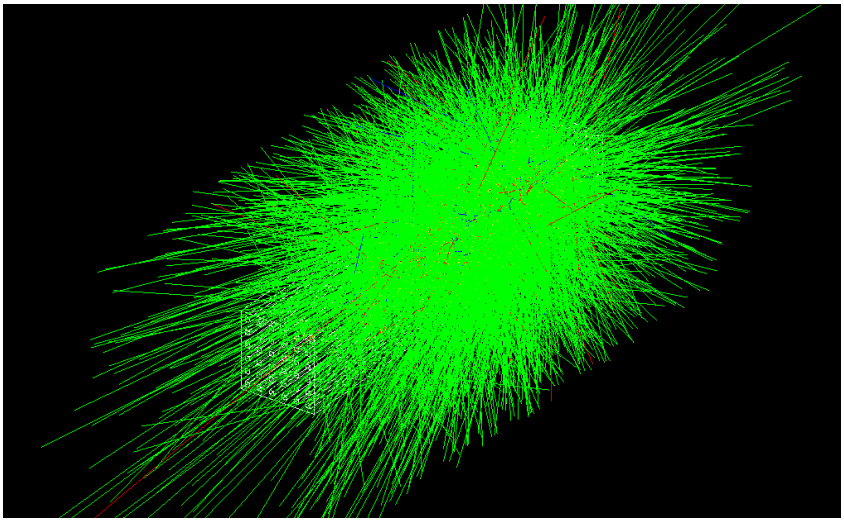

Figure 6. Visualization of calorimeter while beaming on with photons

The irradiation of the module proceeds by photons with energies from 10 MeV to 3 GeV. The development of electromagnetic showers in this element is shown in Figure 6. Photons are shown in green, the interaction points are shown in yellow, electrons and positrons are shown in red.

The most straightforward way to analyze the data is with ROOT. It can get the energy distribution and information about radiation lengths.

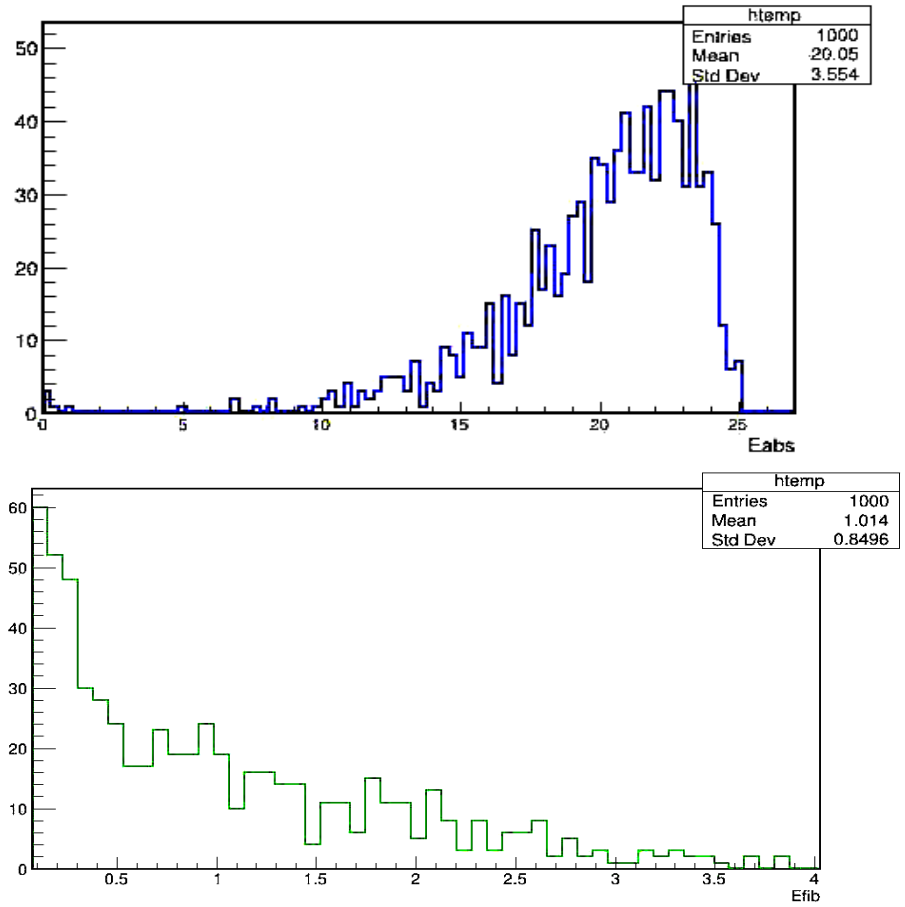

Figure 7. Energy distribution in calorimeter (while beaming on with photons in E=25 MeV)

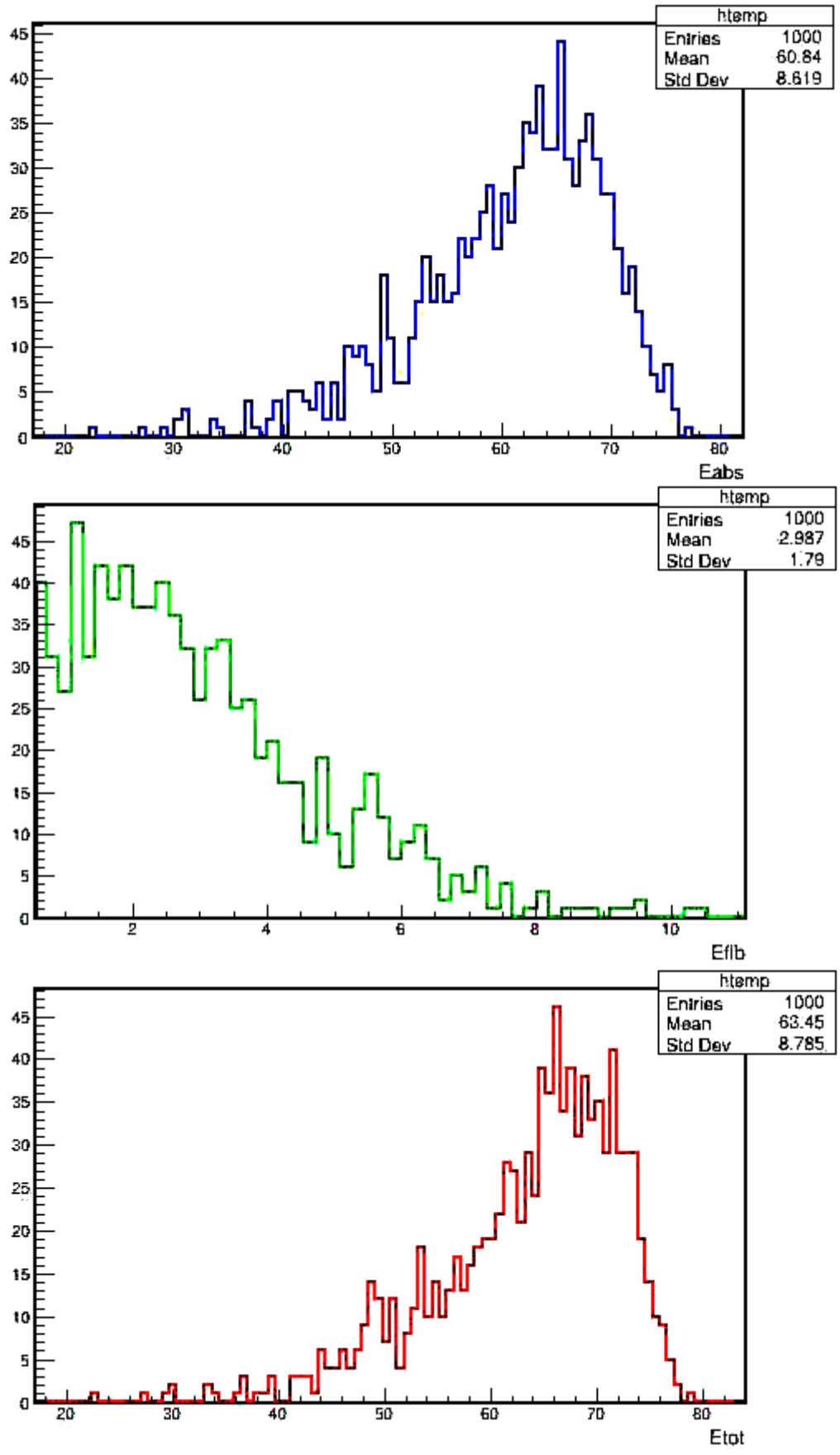

Figure 8. Energy distribution in calorimeter (while beaming on with photons in E=80 MeV)

Conclusion

From the presented graphs (7,8) it can be seen that energy resolution depends on their energy. So if photon with less energy beams on target, then resolution of calorimeter and probability earn of fibers are less value. While beaming on with high energy photons, this effect isn't seen.

References

1. J.F. Owens, Rev. Mod. Phys. 59, 465 (1997).
2. W. Vogelsang et al., J. Phys. G 23, A1 (1997).
3. WA98 Collaboration (M.M. Aggarwal et al.), arXiv:nucl- ex/0006007.
4. P.V. Chliapnikov et al., Phys. Lett. B 141, 276 (1984).
5. M.N. Ukhanov et al., IHEP preprint 86-195, Protvino, (1986).
6. S. Banerjee et al., Phys. Lett. B 305, 182 (1993).
7. A. Belogianni et al., Phys. Lett. B 408, 487 (1997).
8. F. Botterweck et al., Z. Phys. C 51, 541 (1991).
9. DELPHI Collaboration (J. Abdallah et al.), Eur. Phys. J. C 47, 273 (2006).
10. DELPHI Collaboration (J. Abdallah et al.), Eur. Phys. J. C 57, 499 (2008).
11. P. Lichard, L. Van Hove, Phys. Lett. B 245, 605 (1990).
12. E.V. Shuryak, Phys. Lett. B 231, 175 (1989).
13. M.K. Volkov et al., Phys. Lett. B 424, 235 (1998).
14. M.K. Volkov et al., Yad. Fiz. 62, 133 (1999).
15. S. Barshay, Phys. Lett. B 227, 279 (1989).
16. M.K. Volkov, E.S. Kokoulina, E.A. Kuraev, Ukr. J. Phys. 48, 1252 (2003).
17. E.S. Kokoulina, V.A. Nikitin, in Proceedings of International School Seminar "The Actual Problems of Microworld Physics", Gomel, Belarus 2003, Vol. 1 (2005) p. 221.
18. E.S. Kokoulina, V.A. Nikitin, in Proceedings of the XVII International Baldin Seminar on High Energy Physics Problems: Relativistic Nuclear Physics and Quantum Chromodynamics: ISHEPP 2004, edited by A.N. Sissakian,V.V. Burov, A.I. Malakhov (JINR, Dubna, 2005) p. 319.

19. P.F. Ermolov et al., in Proceedings of the XVII International Baldin Seminar on High Energy Physics Problems: Relativistic Nuclear Physics and Quantum Chromodynamics: ISHEPP 2004, edited by A.N. Sissakian, V.V. Burov, A.I. Malakhov (JINR, Dubna, 2005) p. 327.

20. V.V. Avdeichikov et al., JINR-P1-2004-190 (2005).

21. E. Kokoulina, Acta Phys. Pol. B 35, 295 (2004).

22. E. Kokoulina, A. Kutov, Phys. At. Nucl. 71, 1543 (2008).

23. E.S. Kokoulina et al., Phys. At. Nucl. 72, 189 (2009).

24. SVD-2 Collaboration (E.N. Ardashev et al.), IHEP Preprint 2011-4 (2011), http://web.ihep.su/library/ pubs/all-w.htm arXiv:hep-ex/1104.0101.

25. V.A. Nikitin et al., Nonlinear Phenom. Complet Syst. 12, 202 (2010) http://theor.jinr.ru/twiki-cgi/ view/NICA/WebHome.

26. J. Cleymans, K. Redlich, Phys. Rev. C 60, 054908 (1999). 30. F. Becattini, J. Manninen, M. Gazdzicki, Phys. Rev. C 73, 044905 (2006).

27. SVD-2 Collaboration (E.N. Ardashev et al.), Instrum. Exp. Tech. 58, 18 (2015).

28. SVD-2 Collaboration (E. Kokoulina et al.), EPJ Web of Conferences 105, 10005 (2016) arXiv:1510.00517 [nucl-ex].

29. C. Grupen and B. A. Shwartz: Particle Detectors, Second Edition, 2008.

30. A Comprehensive Study on Gamma Rays and Fast Neutron Sensing Properties of GAGOC and CMO Scintillators for Shielding Radiation Applications.

31. “Geant4, a toolkit for the simulation of the passage of particles through matter”, http://geant4.web.cern.ch/geant4/.

32. “Geant4 Material Database” http://geant4-userdoc.web.cern.ch/geant4-userdoc/UsersGuides/ForApplicationDeveloper/html/Appendix/materialNames.html

JOINT INSTITUTE FOR NUCLEAR RESEARCH
Veksler and Baldin laboratory of High Energy Physics

FINAL REPORT ON THE SUMMER STUDENT PROGRAM

Study of feasibility and efficiency of transmutation of the minor actinides Am-241 and Pu-239 in neutron fields

Supervisor:
Tyutyunnikov S.I.

Student:
Fazilat Rasulova, Uzbekistan,
National Research Nuclear
University MEPhI

Participation period:
July 01 – August 17

Dubna, 2019

Abstract

The aim of this work is to study the gamma spectra of the nuclei produced in the ^{237}Np, ^{239}Pu and ^{241}Am targets. The experiments were carried out within the framework of the project “Energy and Transmutation of RAW” and aimed at the solving the problem of the transmutation of actinides – neptunium, americium and plutonium. The aim is to compare the cross section for the capture and fission reactions at different radii of the “Quinta” setup. The acceleration beams consisted of protons and deuteron ions with energies of 0.6, 2, 4, and 8 GeV, respectively. The technique is based on measurements of gamma spectra using germanium detectors.

Introduction

The experiment has been performed in the beam (from the JINR Nuclotron) and in the extracted proton beam with the current of 1 μA and energy of 660 MeV from the Phasotron of the Dzhelepov Laboratory of Nuclear Problems, JINR. This paper presents results of a study of spatial distributions of neutron radiative capture and ^{nat}U fission in the target assembly “Quinta” with a mass of 512 kg of natural metallic uranium irradiated by deuteron beams from the accelerator Nuclotron in the energy range from 1 to 8 GeV with the total number of deuterons on the target ~ 10^{13} at each energy.

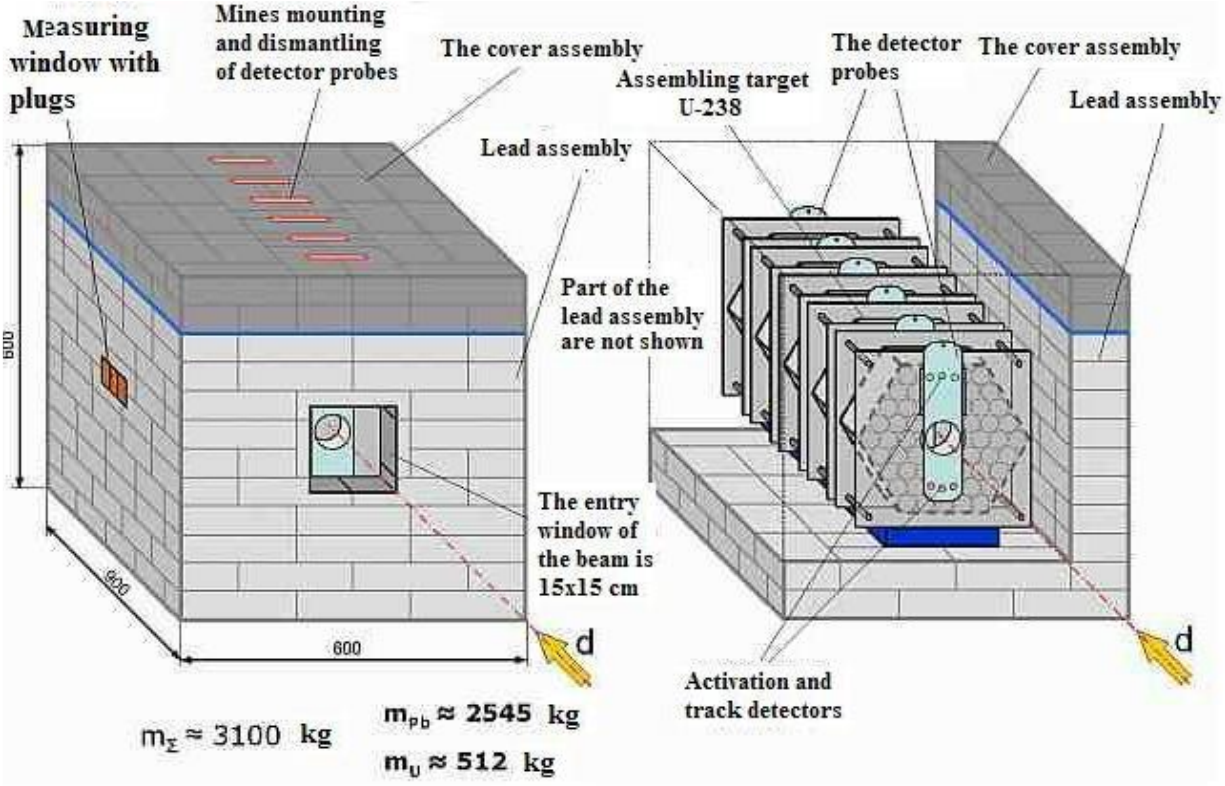

Figure 1. Scheme of the target assembly “Quinta”

The goal of the work is to determine nuclear-physics characteristics of these nuclei, the capture-to-fission cross section ratio, and the cross sections for production of residual nuclei in the targets of ^{238}U, ^{237}Np, ^{241}Am, and ^{239}Pu in the neutron field at the far radius (~200 mm) of the “Quinta” uranium (^{238}U) assembly

irradiated with 660-MeV protons. At the given point the percentage ratio of the low-energy neutrons is the largest, which allows capture reactions to be separated. Gamma spectra of the irradiated targets were measured at a distance of 100 and 200 mm using an HPGe detector with an efficiency of 30% fabricated at IPTP and a filter (50 mm Pb + 2 mm Cd + 2 mm Cu + 2 mm Al).

^{238}U: -The investigation is concerned with the spectrum of ^{239}Np (58 h) resulting from a chain of beta decays:

$$^{238}\mathrm{U(n,\gamma)}^{239}\mathrm{U}\ (23{,}54\ \mathrm{m})\ \beta^- \rightarrow {}^{239}\mathrm{Np}\ (2{,}36\ \mathrm{d})\ \beta^- \rightarrow {}^{239}\mathrm{Pu}.$$

^{237}Np: -Neptunium is one of 15 actinides, produced artificially in power reactor as an energy production by product. Np-237 is its longest living isotope with half-life time $2.144 \cdot 10^6$ y. To get rid of its long livened activity one has to fission it somehow. There's no easy way to do it.

^{239}Pu, ^{241}Am: -The processing of the data resulted in observing short-lived residual nuclei with a half-life $T_{1/2}$ > 5 min among the products of each target nucleus.

Analysis of the spatial distributions of neutron radiative capture to fission ratios (spectral indices), the accuracy of which is substantially higher than the rest of the studied observables (due to the absence of systematic errors of monitoring of deuteron numbers on the target), indicates softening of the neutron spectrum at offset from the axis to the periphery of the uranium target. The degree of this softening increases when adding a lead blanket to the target assembly.

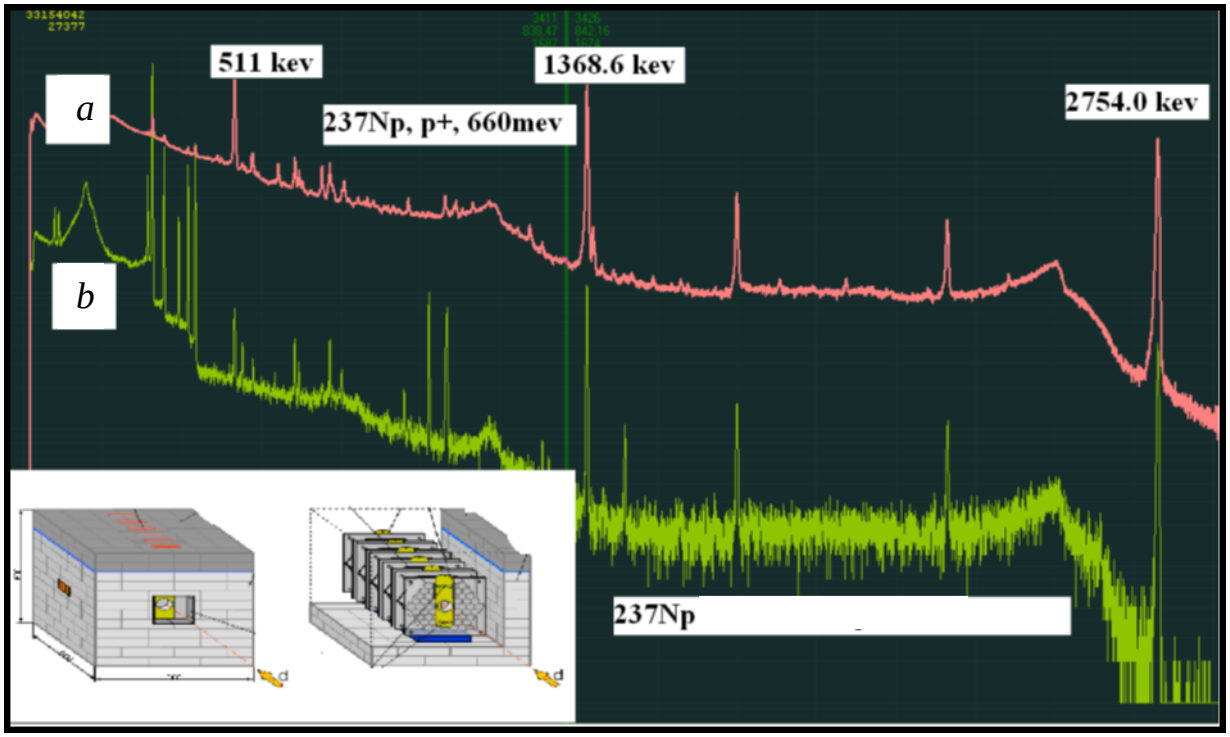

Figure 2. ^{237}Np target after their irradiation by the "Quinta" neutron field: *a)* at a near radius; *b)* at a far radius (intense peaks of ^{234}Pa are visible)

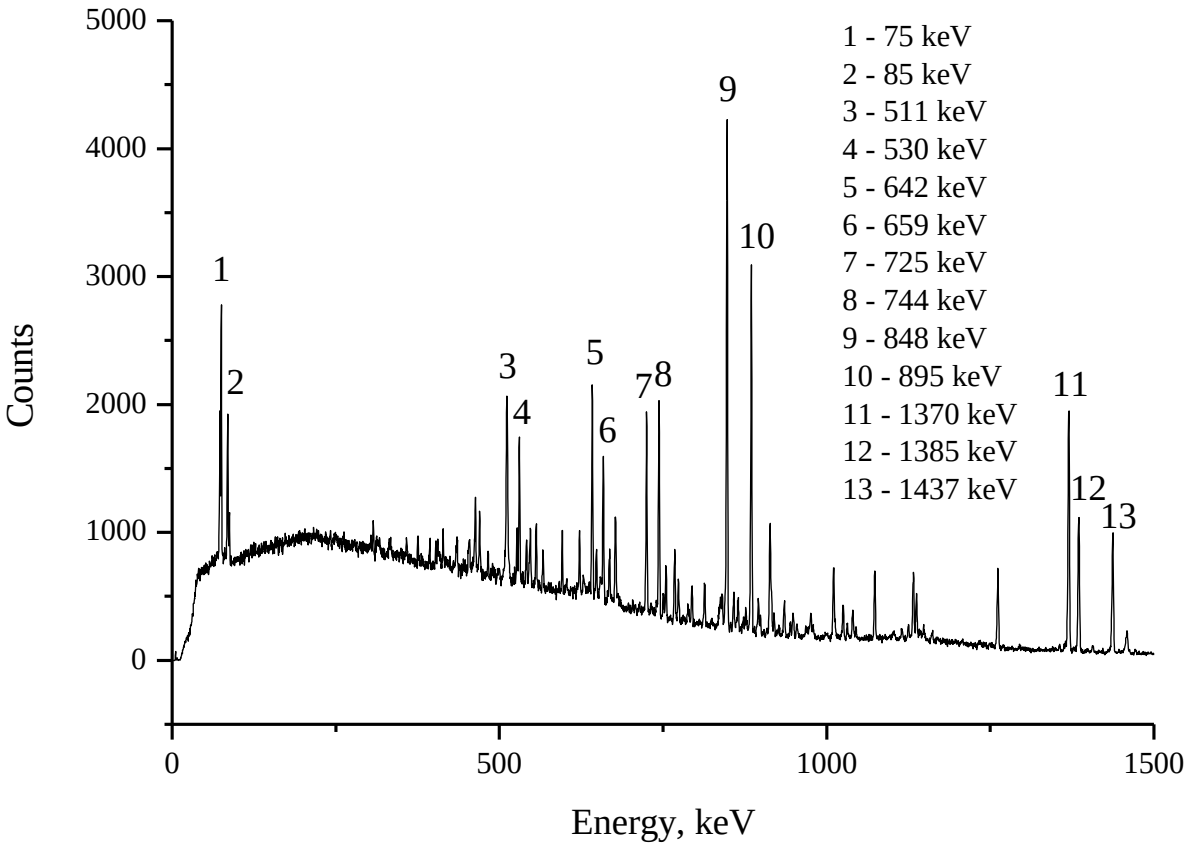

Figure 3. ^{239}Pu target after their irradiation by the "Quinta" neutron field

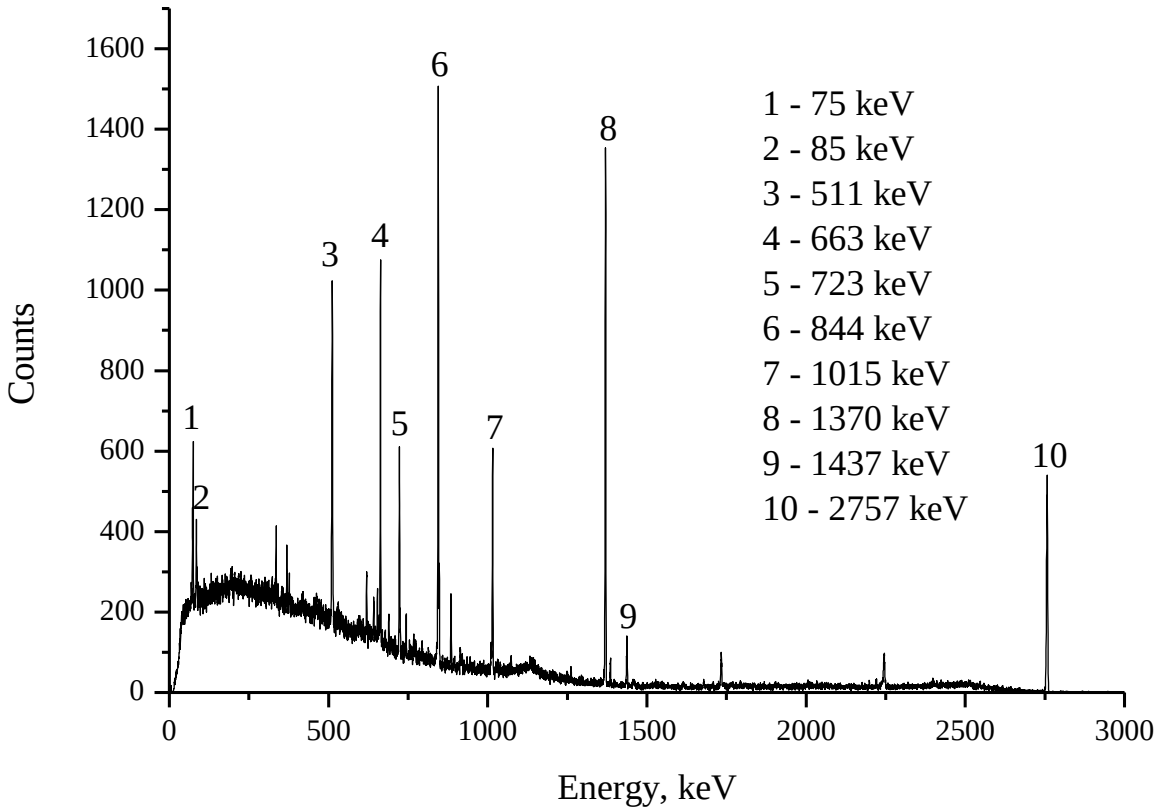

Figure 4. ^{241}Am target after their irradiation by the "Quinta" neutron field

The germanium (Ge) detector is a counting detector and is the instrument that we will be using to count individual gamma emissions from samples. Gamma emissions are direct indicators of decay events. Since we are only using one detector, we are missing most of the decays because they emit gammas in every direction. We already know going into the experiment that our detector will have a total efficiency of no more than 3 or 4 percent and that its peak efficiency will be even lower.

The data acquisition program GammaMCA, showed a full spectrum and included a library of all known radionuclide decay emissions. Wherever there was a peak, the program displayed the energy and what nuclide corresponded to that specific peak, not taking into account the effects of electron escape, cascading effects or the background.

Energy readings were taken straight from the GammaMCA program and peak efficiencies were calculated using the following formula:

$$\varepsilon = S/I$$

The I – gamma term refers to the branching ratios of specific gamma energies; S – counts

In order to identification of nuclides values of efficiency can be found by experimental methods. For determining of efficiency of detector are used nuclide ^{152}Eu, which has known all lines in the spectrum. Via values of efficiency were found intensity of gamma-quantum of ^{154}Eu, results have to check and compare with tabular values.

Table 1. Calculation of efficiency of detectors

№	Energy, keV	Counts		Intensity (table value)	Efficiency		Trend line	
		Detector №1	Detector №2		Detector №1	Detector №2	Detector №1	Detector №2
1	121,8	218988	708726	28,58	7662,3	24798	$Eff(E)=-7,3+13,5*E-5,2*E^2+0,63*E^3$	$Eff(E)=-6,15+12,8*E-4,94*E^2+0,6*E^3$
2	244,7	45723	148291	7,583	6030	19556		
3	344,3	121800	386367	26,5	4596	14580		
4	779	29084	94913	12,942	2247,3	7334		
5	867,4	8729	28906	4,245	2056,3	6809,4		
6	964,1	27436	90619	14,605	1878,5	6205		
7	1086	17784	56781	10,207	1742,3	5563		
8	1112,1	23331	76068	13,644	1710	5575,2		
9	1213	2351	7391	1,422	1653	5197,6		
10	1299	2481	8331	1,623	1529	5133,1		
11	1408	29393	96519	21,07	1395	4580,8		

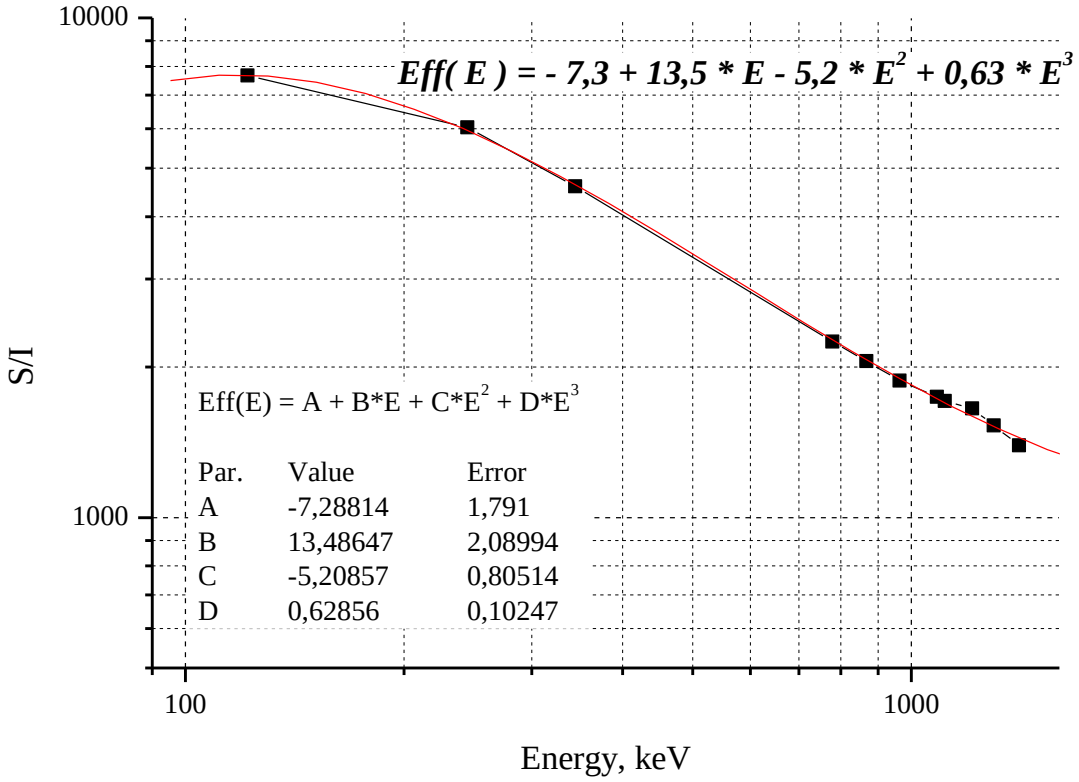

Figure 4. Efficiency of detector №1

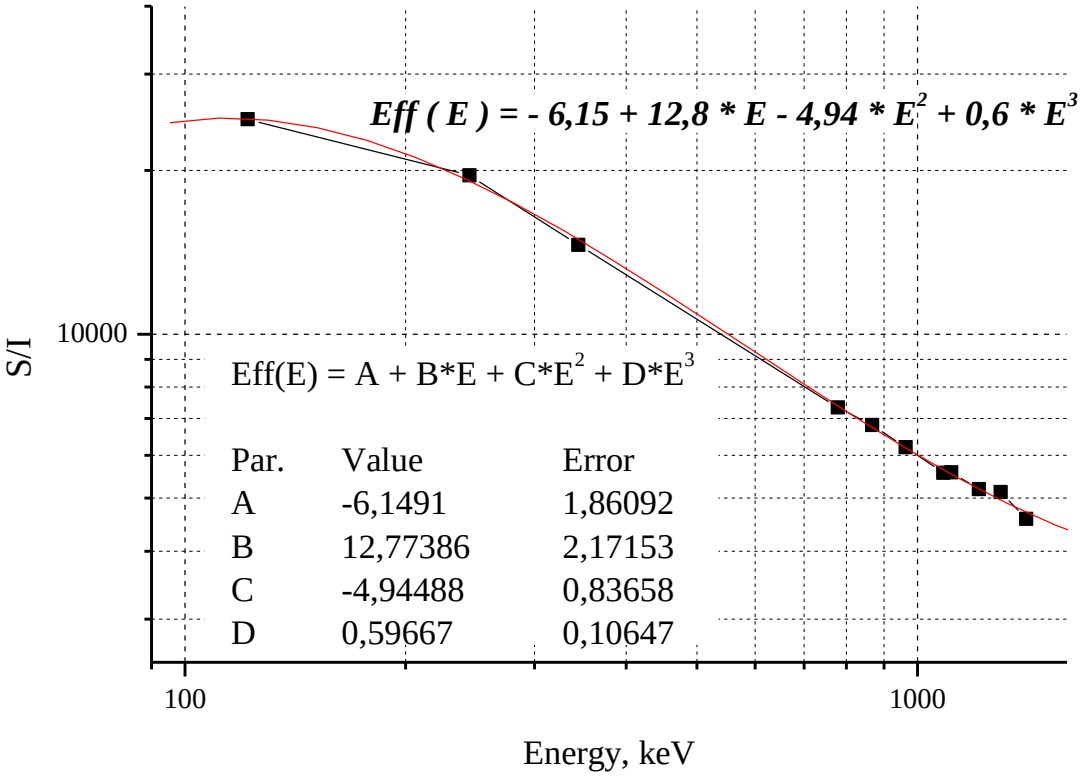

Figure 5. Efficiency of detector №2

Knowing the value of efficiency, can determine the intensity of gamma quanta. This expands the possibility of finding the nuclide obtained by irradiating the target. Eu-154 is used nuclide for checking of efficiency of detector, can see experimental results coincide with tabular values.

Table 2. Calculation of intensity of gamma-quantum

№	Energy, keV	Intensity obtained at the first detector	Intensity obtained at the second detector	Intensity (tabular values)
1	123,071	41,57632	40,94072	40,79
2	247,925	6,995422	6,721039	6,95
3	591,763	4,807033	4,994608	4,99
4	692,421	1,848733	1,766761	1,802
5	723,304	20,02627	19,69846	20,22
6	756,763	4,618939	4,670885	4,57
7	873,190	12,26427	12,12152	12,27
8	996,262	10,42707	10,72386	10,6
9	1004,725	17,93827	18,06751	18,01
10	1274,436	34,28929	34,28999	35,19
11	1596,495	1,717187	1,891407	1,798

Summary

1. Student met with the experiments of the project “Energy and Transmutation of RAW”.
2. In order to identification of nuclides in targets after their irradiation by the “Quinta” neutron field values of efficiency were found by experimental methods. Via values of efficiency were found intensity of gamma-quantum of ^{154}Eu, results were checked and compared with tabular values.
3. The thesis Tyutyunnikov S.I., Stegailov V.I., Rasulova F.A., Kriashko I.A. “^{241}Am and ^{239}Pu targets in the “Quinta” neutron field. Isomerism of formed nuclei” was written based on the results.

References

1. K. Debertin and R. G. Helmer, Gamma- and X-Ray Spectrometry with Semiconductor Detectors, North Holland Publishing Company, Elsevier Science Publishers B. V., Amsterdam, The Netherlands, (1988)
2. S.Kilim et al. //Nucleonica. 2018. V.63(1).P.17
3. S.I.Tyutyunnikov//24-Inter. Baldin Seminar, Russia, Dubna, September, 17-22, 2018.
4. A.A.Smirnov, V.I.Stegailov, S.I.Tyutyunnikov, et al. // “Nucleus2015”, St-Petersb. P.257.

Acknowledgments

I express my deep gratitude for the help and advice in the work Tyutyunnikov S.I., Stegailov V.I., Kokoulina E.S. and to the organizers of the summer student practice of JINR for a great time and useful experience. Thank you.